

Graphene-Silicon Heterojunction Photodetector with plasmonic metasurface for graphene gating and optical absorption enhancement

Laiwen Yu
College of Optical Science and
Engineering
Zhejiang University
Hangzhou, China
11930055@zju.edu.cn

Jingshu Guo
College of Optical Science and
Engineering
Zhejiang University
Hangzhou, China
jsguo@zju.edu.cn

Chayue Liu
College of Optical Science and
Engineering
Zhejiang University
Hangzhou, China
11730043@zju.edu.cn

Hengtai Xiang
College of Optical Science and
Engineering
Zhejiang University
Hangzhou, China
12130065@zju.edu.cn

Daoxin Dai
College of Optical Science and
Engineering
Zhejiang University
Hangzhou, China
dxdai@zju.edu.cn

Abstract—We demonstrate a plasmonically enhanced graphene-silicon heterojunction photodetector with high speed. The plasmonic metasurface structure works as gate electrode for graphene doping tuning and optical absorption enhancement simultaneously, yielding a ~ 3.6 -fold increase in responsivity.

Keywords—silicon photonics, graphene, heterojunction, photodetector

I. INTRODUCTION

Recently, graphene has shown great potential for realizing photodetection because of excellent optoelectronic properties, including the broadband absorption [1] and CMOS compatibility [2] with silicon. Due to the lack of a band gap, the metal-graphene-metal (MGM) structures often achieve a good responsivity and high speed with a large dark current or thermal noise [3], [4]. A popular approach to reduce dark currents is to introduce graphene silicon heterojunction (GSH) structures [5]–[7], but few devices exhibit high responsivity. In order to improve the reponsivity, photodetectors (PDs) can be enhanced by plasmonic structures, which offer strong subwavelength mode confinement and local field enhancement [3], [8].

In this letter, we presented and fabricated a g GSH PD with plasmonic metasurface for graphene gating and optical absorption enhancement. Compared to conventional surface-illuminated GSH PDs [7], [9], we can tune the work function (WF) of graphene by the top gate atop the dielectric on graphene. For the fabricated plasmonically enhanced GSH PD, the responsivity was improved by ~ 3.6 -fold (Laser Power=14 dBm, $V_{\text{bias}}=-6$ V, $V_{\text{gate}}=2$ V) compared to the PD without plasmonic structure. Moreover, the response of the device to a high frequency has been achieved, which proves that the presented PD can operate a bandwidth of >30 MHz.

II. DESIGN, FABRICATION AND CHARATERIZATION

Fig. 1(a) shows the configuration of the present surface-illuminated GSH PD integrated with the plasmonic metasurface. As Fig. 1(b) shows, the large-area chemical vapor deposition (CVD) grown monolayer of graphene was transferred and patterned on Si to form Graphene-Si Schottky junction, The Al/Au electrode was fabricated on both Si and graphene. A 10-nm-thick Al_2O_3 layer was deposited on the pattern layer of graphene by using an atomic-layer deposition (ALD) process.

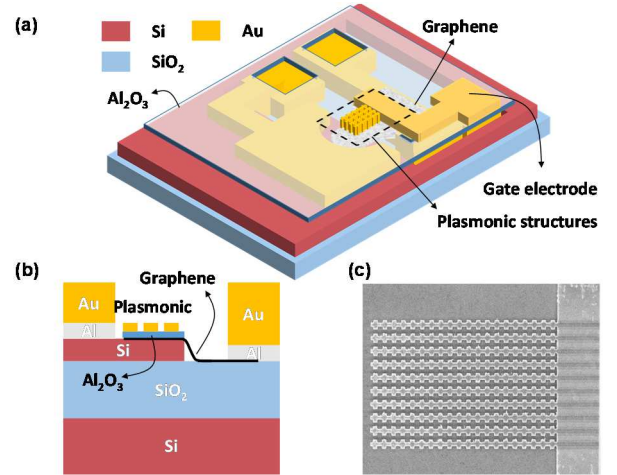


Fig. 1. (a) Schematic configuration of the present GSH photodetector; (b) Cross-sectional view of the device; (c) The SEM image for the fabricated plasmonic metasurface structure.

The metallic metasurface structures with nanoscale gaps were placed on top of the Al_2O_3 layer to enhance light absorption while acting as a top gate electrode to tune the doping of graphene at the same time. Fig. 1(c) shows the SEM image of the fabricated plasmonic metasurface structure.

We simulated and optimized the light absorption in the GSH PD by 3D-FDTD. Figure 2(a) shows the distribution of the light field in graphene plane, from which it can be seen that the energy is mainly concentrated at the edges of the plasmonic structure. Fig. 2(b) shows the absorption ratio of each part. The total optical proportion is derived from the sum of the transmission $\eta(Tr)$, reflection $\eta(Re)$ and the light absorption in metal $\eta(Metal)$ and graphene $\eta(Gr)$:

This work was supported by National Major Research and Development Program (No. 2018YFB2200200); National Science Fund for Distinguished Young Scholars (61725503); National Natural Science Foundation of China (NSFC) (62175216, 61961146003, 91950205); Zhejiang Provincial Natural Science Foundation (LR22F050001); The Fundamental Research Funds for the Central Universities; The Leading Innovative and Entrepreneur Team Introduction Program of Zhejiang (2021R01001).

$$\eta(Total) = \eta(Tr) + \eta(Re) + \eta(Metal) + \eta(Gr) \quad (1)$$

In particular, the transmission and reflection intensity can be obtained from the monitor in the FDTD simulation. For the input power P_0 , the absorption ratio of metal is calculated by:

$$\eta(Metal) = \frac{\iiint P_m(\omega, x, y, z) dx dy dz}{P_0} \quad (2)$$

Here, $P_m(x, y)$ is the metal absorption intensity given by $P_m(\omega, x, y, z) = \frac{1}{2} \omega \cdot \text{Imag}(\epsilon_m) |\vec{E}(x, y, z)|^2$ (W/m³), where $\text{Imag}(\epsilon_m)$ is the imaginary part of the metal permittivity, ω is the angular optical frequency, \vec{E} is the electric fields in the metal area. Similarly, the absorption ratio of graphene is calculated by:

$$\eta(Graphene) = \frac{\iint P_g(x, y) dx dy}{P_0} \quad (3)$$

One has $P_g(x, y) = \frac{1}{2} \text{Real}(\sigma_g) |\vec{E}_t(x, y)|^2$ (W/m²), where $\text{Real}(\sigma_g)$ is the real part of the graphene conductivity, l is the coordinate of the line integral along the graphene surface, \vec{E}_t is the transverse component of the electric field of the launched waveguide mode along the graphene surface (at $z = 0$). One can see that it is close to 100% in the simulation wavelength band, which confirms the correctness of the simulation [4]. Benefiting from the enhanced light absorption of the plasmonic structure, one can achieve a 30% light absorption ratio in graphene. By integrating graphene with silicon, a Schottky junction is formed at the graphene-silicon interface and a built-in electric field is created from the bulk silicon to the graphene [10].

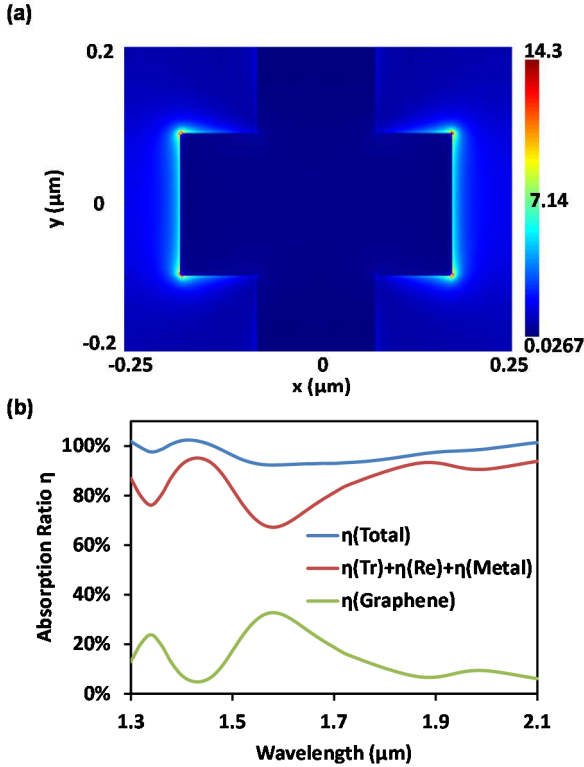


Fig. 2. (a) Optical field distribution in the graphene plane; (b). The optical absorption ratio η for each part, $\eta(Total)$: Total light absorption, $\eta(Tr)$: Transmission absorption ratio, $\eta(Re)$: Reflection absorption ratio, $\eta(Metal)$: Metal absorption ratio, $\eta(Graphene)$: Graphene absorption ratio.

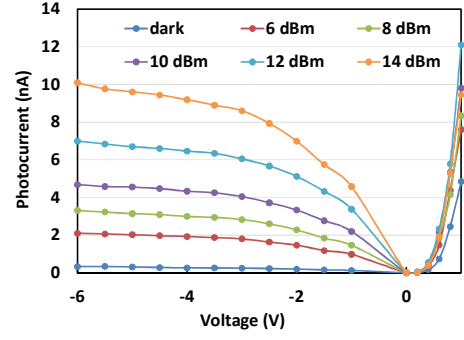


Fig. 3. Measured I-V curves for the GSH PD operating with different optical powers

Fig. 3 shows the current-voltage (I-V) curves of the GSH PD when operating at $\lambda=1550$ nm, with laser power varying from 6 dBm to 14 dBm. It can be seen that the photocurrent increases with increasing optical power, and the device has a photocurrent of ~ 10 nA at a power of 14 dBm with a bias of -6 V.

When introducing the plasmonic structures, as shown in the Fig. 4(a), the photocurrents of the present PD are increased and can be adjusted by the gate voltage. The gate-dependent photoresponse suggests that the graphene doping level is adjusted and the Schottky barrier height is successfully manipulated. As expected, the forward current remains almost constant under illumination, while the reverse current increases with increasing incident optical power due to the generation of photo-carriers at the hetero-junction. The dependence of photocurrent versus optical power is shown in Fig. 4(b) with a bias voltage of -6 V. It can be seen that the photocurrent of GSH PD varies linearly with the increase of optical power, while the photocurrent of the present plasmonic enhanced GSH PD increases ~ 3.6 -fold at an optical power of 14 dBm.

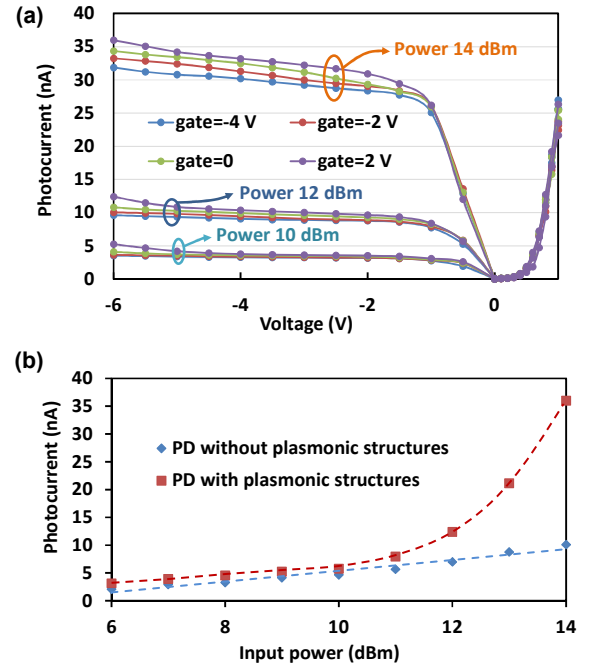


Fig. 4. (a) Measured I-V curves for the plasmonically enhanced GSH PD operating with different optical powers and gate voltages; (b) Measured photocurrents as the optical power increases with/without plasmonic structures.

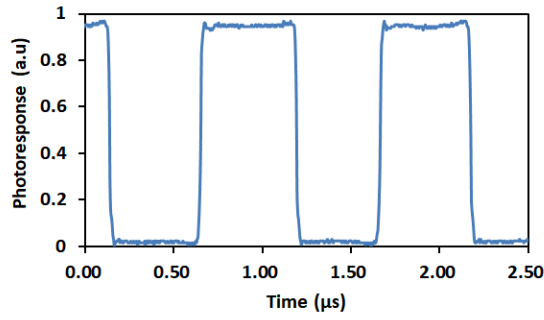


Fig. 5. Normalized photoresponse of the plasmonically enhanced GSH PD, excited by a 1550 nm laser modulated by a 1 MHz square wave.

The photoresponse of the plasmonically enhanced GSH PD was measured by an oscilloscope with a 1 MHz modulated square wave and a bias voltage of -5 V, as shown in Fig. 5. Apparently, this device demonstrates the potential for high speed. The rising time is $<1.2 \times 10^{-8}$ s (limited by the set-ups such as transimpedance amplifier), and the bandwidth is over 30 MHz.

III. CONCLUSION

In conclusion, we have presented and fabricated a plasmonically enhanced graphene-silicon heterojunction photodetector with gate-controlled Schottky barrier height [11]. It has been exhibited that there is the optical enhancement in the structure, thus achieving a higher responsivity. The fast response of the device shows a set-up limited bandwidth of >30 MHz. By optimizing the doping in silicon and improving the fabrication processes, the improved photocurrents are expected in the future.

REFERENCES

- [1] B. Y. Zhang, T. Liu, B. Meng, X. Li, G. Liang, X. Hu, and Q. J. Wang, "Broadband high photoresponse from pure monolayer graphene photodetector," *Nat. Commun.*, vol. 4, no. 1, p. 1811, May 2013.
- [2] A. Pospischil, M. Humer, M. M. Furchi, D. Bachmann, R. Guider, T. Fromherz, and T. Mueller, "CMOS-compatible graphene photodetector covering all optical communication bands," *Nat. Photonics*, vol. 7, no. 11, pp. 892–896, Nov. 2013.
- [3] P. Ma, Y. Salamin, B. Baeuerle, A. Josten, W. Heni, A. Emboras, and J. Leuthold, "Plasmonically Enhanced Graphene Photodetector Featuring 100 Gbit/s Data Reception, High Responsivity, and Compact Size," *ACS Photonics*, vol. 6, no. 1, pp. 154–161, Jan. 2019.
- [4] J. Guo, J. Li, C. Liu, Y. Yin, W. Wang, Z. Ni, Z. Fu, H. Yu, Y. Xu, Y. Shi, Y. Ma, S. Gao, L. Tong, and D. Dai, "High-performance silicon-graphene hybrid plasmonic waveguide photodetectors beyond 1.55 μm ," *Light Sci. Appl.*, vol. 9, no. 1, p. 29, Feb. 2020.
- [5] J. Guo, C. Liu, L. Yu, H. Xiang, Y. Xiang, and D. Dai, "High-Speed Graphene-Silicon-Graphene Waveguide PDs with High Photo-to-Dark-Current Ratio and Large Linear Dynamic Range," *Laser Photonics Rev.*, p. 2200555, Feb. 2023.
- [6] X. Wang, Z. Cheng, K. Xu, H. K. Tsang, and J.-B. Xu, "High-responsivity graphene/silicon-heterostructure waveguide photodetectors," *Nat. Photonics*, vol. 7, no. 11, pp. 888–891, Nov. 2013.
- [7] H. Selvi, E. W. Hill, P. Parkinson, and T. J. Echtermeyer, "Graphene-silicon-on-insulator (GSOI) Schottky diode photodetectors," *Nanoscale*, vol. 10, no. 40, pp. 18926–18935, 2018.
- [8] M. L. Brongersma, "Plasmonic Photodetectors, Photovoltaics, and Hot-Electron Devices," *Proc. IEEE*, vol. 104, no. 12, pp. 2349–2361, Dec. 2016.
- [9] A. Levi, M. Kirshner, O. Sinai, E. Peretz, O. Meshulam, A. Ghosh, N. Gotlib, C. Stern, S. Yuan, F. Xia, and D. Naveh, "Graphene Schottky Varactor Diodes for High-Performance Photodetection," *ACS Photonics*, vol. 6, no. 8, pp. 1910–1915, Aug. 2019.
- [10] C. Liu et al., "Silicon/2D-material photodetectors: from near-infrared to mid-infrared," *Light Sci. Appl.*, vol. 10, no. 1, p. 123, Jun. 2021.
- [11] H. Yang et al., "Graphene Barristor, a Triode Device with a Gate-Controlled Schottky Barrier," *Science*, vol. 336, no. 6085, pp. 1140–1143, Jun. 2012.